





# vEEGNet: A New Deep Learning Model to Classify and Generate EEG

Alberto Zancanaro<sup>1</sup><sup>a</sup>, Italo F. Zoppis<sup>2</sup><sup>b</sup>, Sara L. Manzoni<sup>2</sup><sup>c</sup> and Giulia Cisotto<sup>1,2</sup><sup>d</sup>

<sup>1</sup>Department of Information Engineering, University of Padova, via Gradenigo 6/b, Padova, Italy

<sup>2</sup>Department of Informatics, Systems, and Communications, University of Milano-Bicocca, viale Sarca 336, Milan, Italy

**Keywords:** AI, Deep Learning, Variational Autoencoder, EEG, Machine Learning, Brain, Classification, Latent Space, Inter-Subject Variability.


**Abstract:** The classification of EEG during motor imagery (MI) represents a challenging task in neuro-rehabilitation. In 2016, a deep learning (DL) model called EEGNet (based on CNN) and its variants attracted much attention for their ability to reach 80% accuracy in a 4-class MI classification. However, they can poorly explain their output decisions, preventing them from definitely solving questions related to inter-subject variability, generalization, and optimal classification. In this paper, we propose vEEGNet, a new model based on EEGNet, whose objective is now two-fold: it is used to classify MI, but also to reconstruct (and eventually generate) EEG signals. The work is still preliminary, but we are able to show that vEEGNet is able to classify 4 types of MI with performances at the state of the art, and, more interestingly, we found out that the reconstructed signals are consistent with the so-called motor-related cortical potentials, very specific and well-known motor-related EEG patterns. Thus, jointly training vEEGNet to both classify and reconstruct EEG might lead it, in the future, to decrease the inter-subject performance variability, and also to generate new EEG samples to augment small datasets to improve classification, with a consequent strong impact on neuro-rehabilitation.


## 1 INTRODUCTION


Electroencephalography (EEG)-based classification represents a challenging and critical problem in many applications, e.g., neuroscience and brain-computer interface (BCI) to support the diagnosis of movement disorders and motor rehabilitation (Cisotto et al., 2022). Particularly, besides promising achievements in supporting disabled individuals, neurorobotics and BCI systems (Beraldo et al., 2022) are still poorly performing in many tasks, e.g., motor imagery (MI) classification. There exist several machine learning (ML) and deep learning (DL) models to classify EEG of imagined movements: filter-bank common spatial pattern (FBCSP) (Kai Keng Ang et al., 2008) is the standard ML model, very common in BCI applications where it is used also in real-time. More recently, convolutional neural networks (CNN) have gained a lot of attention as architectures particularly good in classifying EEG. In 2016, EEGNet, an architecture made of 2 blocks, each one composed of


2 convolutional layers and a fully-connected layer, was published by (Lawhern et al., 2016). Given its success in classifying EEG in different classes of movements (both executed and imagined), a number of variants were presented, including Temporary Constrained Sparse Group Lasso enhanced EEGNet (TSGL-EEGNet) (Deng et al., 2021), Multibranch Shallow CNN (MBShallow ConvNet) (Altuwaijri and Muhammad, 2022), MI-EEGNet (Riyad et al., 2021), Quantized EEGNet (Q-EEGNet) (Schneider et al., 2020), *DynamicNet* (Zancanaro et al., 2021), and other general-purpose CNN models, namely Channel-wise CNN (CW-CNN) (Sakhavi et al., 2018), Densely Feature Fusion CNN (DFFN) (Li et al., 2019a), and the Monolithic Network (Olivas and Chacon, 2018). They differ from each other by a more (e.g., MI-EEGNet) or less (e.g., EEGNet) invasive pre-processing of the EEG signal, by their architectures with single or multiple EEGNet *units* combined to extract one or a few sets of artificial features (e.g., TSGL-EEGNet and MBShallow ConvNet), and by their feasibility in running on portable devices (e.g., Q-EEGNet).

They achieve accuracies in the range of 70% to 80% in a 4-class MI classification. However, they

<sup>a</sup> <https://orcid.org/0000-0002-5276-7030>

<sup>b</sup> <https://orcid.org/0000-0001-7312-7123>

<sup>c</sup> <https://orcid.org/0000-0002-6406-536X>

<sup>d</sup> <https://orcid.org/0000-0002-9554-9367>

cannot, or poorly, relate their classification decisions with well-known EEG patterns or biomarkers.

In this paper, we aim to propose our own DL model, named as vEEGNet, whose objective is two-fold: on one side, the model is used to classify EEG signals obtained during the participant's MI of different body segments (i.e., one hand, the feet, or the tongue); on the other side, the model is enriched by a generative module that is able to reconstruct some specific EEG components, strongly related to MI. vEEGNet consists of two learning modules, i.e., an unsupervised representation learning module, and a supervised module. The first one is formed by a variational auto-encoder (VAE) (Kingma and Welling, 2013; Zancanaro et al., 2022; Li et al., 2019b), while the second is implemented using a feed-forward neural network (FFNN). In the VAE, we exploit EEGNet as an encoder (and, conversely, its mirrored version as a decoder) to extract a compact and highly informative representation of the EEG. The encoder extracts a compact and latent representation of the EEG that is later used by the FFNN to classify the EEG into four different classes of movement. At the same time, that representation made it possible to generate new synthetic EEG samples. To take advantage of this combined approach, vEEGNet was trained by minimizing a joint loss function given by the sum of the VAE loss and the classifier loss.

To assess the performance of vEEGNet as classifier, we tested it on the public *dataset 2a* from the BCI competition IV (containing EEG during four types of imagined movements) and compared the results with other models based on EEGNet that were previously employed to classify the same dataset. We show that vEEGNet reaches comparable classification accuracies and Cohen's  $\kappa$  score as the state of the art (approximately ranging between 70% and 80%). Then, we investigated its ability to decode a multi-channel EEG from its latent representation and we might speculate that our model is able to reconstruct a particular low-frequency well-known component of the EEG that is related to any executed or imagined movement, i.e., the motor related cortical potential (MRCP). However, this contribution is still preliminary and, as such, a number of limitations and open challenges are also discussed, and will need further investigations. Nevertheless, this paper represents a promising way to shed more light on the ability of DL models to solve very complex tasks, such as recognizing different imagined movements from an EEG, providing a link to common neurophysiological patterns that the model might be able to identify and also generate. Furthermore, this paper can contribute to the research question of how to eventually augment

EEG datasets, that typically suffer from limited sizes, preventing DL models to reach satisfactory levels of robustness and generalization.

The rest of this paper is organized as follows: Section 2 describes the VAE theory and introduces the vEEGNet model. Section 3 presents the classification results with respect to other CNN or EEGNet-based models, and discusses the reconstruction and generative potentialities of vEEGNet. Finally, section 4 concludes the paper and paves the way toward new promising future directions.

## 2 MATERIALS AND METHODS

### 2.1 Variational Autoencoder

VAE is an effective encoding-decoding DL approach that provides a structured latent space to be used for random sampling and interpolation (Kingma and Welling, 2013). These properties have led to efficient implementations of VAEs for several unsupervised and semi-supervised learning problems (see e.g., (Hinton and Salakhutdinov, 2006; Li et al., 2019b; Zancanaro et al., 2022)). In probabilistic terms, a VAE is able to learn a variational (approximate posterior) distribution  $q_\phi(\mathbf{z}|\mathbf{x})$  of latent variables  $\mathbf{z}$ , given the observations  $\mathbf{x}$ , as well as a generative model  $p_\theta(\mathbf{x}|\mathbf{z})$  (Blei et al., 2017). This task is obtained using an encoder-decoder pair of deep networks parametrized by  $\phi$  and  $\theta$ , respectively. The training consists of the minimization (w.r.t. parameters  $\phi$  and  $\theta$ ) of the VAE loss,  $\mathcal{L}_{VAE}$ . Typically, the VAE loss is expressed in terms of evidence lower bound (ELBO) for the (evidence) probability  $p(\mathbf{x})$ , namely  $\mathcal{L}(\theta, \phi; \mathbf{x})$ :  $\mathcal{L}_{VAE} = -\mathcal{L}(\theta, \phi; \mathbf{x})$ , provided that

$$\mathcal{L}(\theta, \phi; \mathbf{x}) = \mathbb{E}_{q_\phi(\mathbf{z}|\mathbf{x})} \left( \log \frac{p_\theta(\mathbf{x}, \mathbf{z})}{q_\phi(\mathbf{z}|\mathbf{x})} \right) \quad (1)$$

Thus, for the VAE training, minimizing  $\mathcal{L}_{VAE}$  means maximizing the ELBO for  $p(\mathbf{x})$ . The gap between  $p(\mathbf{x})$  and  $\mathcal{L}(\theta, \phi; \mathbf{x})$  can be best expressed by considering the Kullback-Leibler divergence ( $\mathcal{KL}$ ) between the variational  $q_\phi(\mathbf{z}|\mathbf{x})$  and posterior  $p_\theta(\mathbf{x}|\mathbf{z})$  distributions, which turns to be

$$\mathcal{KL}[q_\phi(\mathbf{z}|\mathbf{x})||p_\theta(\mathbf{x}|\mathbf{z})] = -\mathcal{L}(\theta, \phi; \mathbf{x}) + p(\mathbf{x}) \quad (2)$$

Since  $\mathcal{KL}[q_\phi(\mathbf{z}|\mathbf{x})||p_\theta(\mathbf{x}|\mathbf{z})] \geq 0$ , one arrives at the lower bound  $\mathcal{L}(\theta, \phi; \mathbf{x}) \leq p(\mathbf{x})$ . Similarly, ELBO can be also formulated as

$$\mathcal{L}(\theta, \phi; \mathbf{x}) = \mathbb{E}_q(p_\theta(\mathbf{x}|\mathbf{z})) - \mathcal{KL}[q_\phi(\mathbf{z}|\mathbf{x})||p(\mathbf{z})] \quad (3)$$

In this way, the second term  $\mathcal{KL}[q_\phi(\mathbf{z}|\mathbf{x})||p(\mathbf{z})]$  acts as a regularizer, thus penalizing those *surrogate* distributions,  $q_\phi(\mathbf{z}|\mathbf{x})$ , too far away from the predefined  $p(\mathbf{z})$ .

## 2.2 vEEGNet

In this work, we devised a new combined model based on a VAE (Kingma and Welling, 2013; Li et al., 2019b) and our previous implementation of EEGNet (Zancanaro et al., 2021), as represented in Fig. 1. Particularly, the model exploits EEGNet in the VAE, for both encoding and decoding the EEG samples, while an FFNN is used for the classification. As a consequence, the model consists of two different mechanisms, ruled by an unsupervised and a supervised learning, respectively, as further explained in the following.

### 2.2.1 Unsupervised Mechanism

The unsupervised mechanism (i.e., the VAE) exploits the EEGNet architecture to supply the latent distribution  $q_\phi(\mathbf{z}|\mathbf{x})$  as well as the posterior  $p_\theta(\mathbf{x}|\mathbf{z})$ . We assumed isotropic Gaussian distribution for both the prior  $p(\mathbf{z})$  and the approximate posterior,  $q_\phi(\mathbf{z}|\mathbf{x})$ , i.e.,

$$p(\mathbf{z}) = \mathcal{N}(\mathbf{0}, \mathbf{I}) \quad (4)$$

$$q_\phi(\mathbf{z}|\mathbf{x}) = \mathcal{N}(\mathbf{z}; \mu(\mathbf{x}; \phi), \sigma^2(\mathbf{x}; \phi)\mathbf{I}) \quad (5)$$

where  $\mu(\mathbf{x}; \phi)$  and  $\sigma(\mathbf{x}; \phi)$  are the functions implemented by the vEEGNet encoder to encode the mean and the (diagonal) covariance matrix of the Gaussian distribution. With these assumptions,  $\mathcal{KL}[q_\phi(\mathbf{z}|\mathbf{x})||p(\mathbf{z})]$  (the regularization term defined in Section 2.1) can be directly expressed in the compact analytical form (Kingma and Welling, 2013):

$$\mathcal{L}_{KL} = \mathcal{KL}[q_\phi(\mathbf{z}|\mathbf{x})||p(\mathbf{z})] = \frac{1}{2} \sum_{i=1}^d (\sigma_i^2 + \mu_i^2 - 1 - \log(\sigma_i^2)) \quad (6)$$

where  $\mu_i$  and  $\sigma_i^2$  are the predicted mean and variance values of the corresponding  $i$ -th latent component of  $\mathbf{z}$ . The vEEGNet encoder implements a standard EEGNet with its usual blocks, i.e., a temporal convolution, a spatial convolution, and a separable convolution. Lastly, the output is flattened and passed through a fully-connected layer. From the vEEGNet encoder's output (i.e., giving  $q_\phi(\mathbf{z}|\mathbf{x})$ ), we sample a vector, say  $\mathbf{z}_1$ <sup>1</sup>, and provide it as the input for the vEEGNet decoder that has the final aim to reconstruct the original EEG signal. The vEEGNet decoder implements

<sup>1</sup>Because this operation is not differentiable this is typically obtained with reparametrization by setting  $\mathbf{z}_1 = \mu + \sigma \cdot N(\mathbf{0}, \mathbf{1})$ .

a mirrored EEGNet structure using transposed convolutions (in place of the standard convolution) and up-sample layers (in place of the pooling layers). In both the vEEGNet encoder and the decoder, batch normalization and dropout layers were added to increase performance and stability during training.

### 2.2.2 Supervised Mechanism

The supervised mechanism is given by an FFNN that classifies the EEG into 4 different classes. The FFNN consists of an input layer (128 neurons), followed by one hidden layer (64 neurons) and one output layer (4 neurons) for the target. In vEEGNet, a second vector  $\mathbf{z}_2 = [\boldsymbol{\mu}, \boldsymbol{\sigma}^2]$  is obtained by concatenating the output of the encoder, i.e. the parameters vectors  $\tilde{\boldsymbol{\mu}} = \boldsymbol{\mu}(\mathbf{x}; \boldsymbol{\phi})$  and  $\tilde{\boldsymbol{\sigma}} = \boldsymbol{\sigma}(\mathbf{x}; \boldsymbol{\phi})$ . This new vector is fed into the classifier to output the predicted class  $\tilde{y}$ . For the classifier, we used the negative log-likelihood loss function defined as:

$$\mathcal{L}_{clf} = -\log(\tilde{\mathbf{y}}) \cdot \mathbf{y} \quad (7)$$

where  $\log(\tilde{\mathbf{y}})$  are the log probabilities of possible labels related to input  $\mathbf{x}$ , and  $\mathbf{y}$  is a one hot encoded vector of the true labels of input  $\mathbf{x}$ .

Overall, vEEGNet aims to minimize the loss function  $\mathcal{L}_{Total}$  given by the sum of the VAE loss function and the classifier loss function ( $\mathcal{L}_{clf}$ ), as follows:

$$\mathcal{L}_{Total} = \mathcal{L}_{VAE} + \mathcal{L}_{clf}.$$

## 3 RESULTS AND DISCUSSION

### 3.1 Dataset and vEEGNet Implementation

To test the reliability of vEEGNet as a model for EEG-based MI, we used it to classify the 4 different MI tasks included in the public *dataset 2a* of the IV BCI competition (Blankertz et al., 2007). The latter includes 22-channel EEG recordings from 9 subjects repeatedly performing MI of either right or left hand, feet or tongue. A set of 288 trials were available for each subject for the training, and another set of 288 trials for the test set for each subject. The EEG data have been previously filtered with a 0.5 – 100Hz band-pass filter and a notch filter at 50 Hz. In line with other works (Riyad et al., 2021; Lawhern et al., 2016) and our previous paper (Zancanaro et al., 2021), we down-sampled the EEG signals at 128Hz. Then, from each MI repetition, one 4s multi-channel EEG segment was extracted, thus obtaining a  $22 \times 512$  data matrix. We implemented

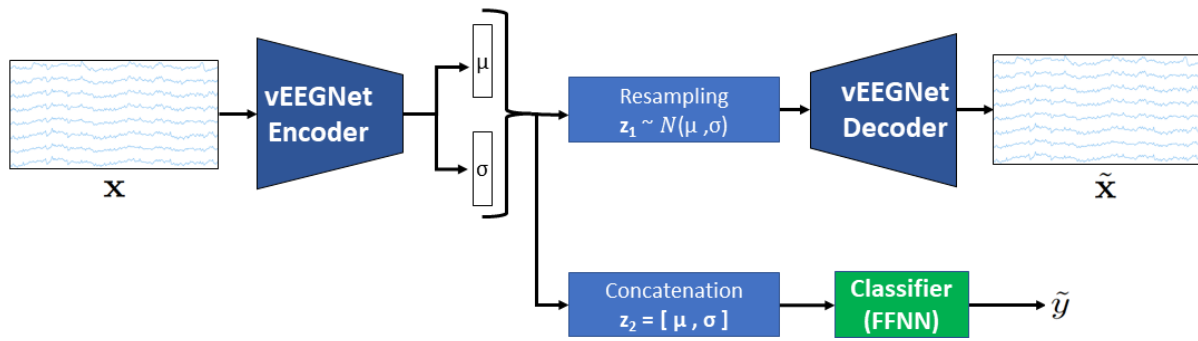


Figure 1: vEEGNet architecture.

vEEGNet in PyTorch<sup>2</sup> and we trained it using RTX 2070, 500 epochs, AdamW optimizer (Loshchilov and Hutter, 2019), a learning rate of 0.001, and a weight decay of 0.00001. The total number of trainable parameters is 61476, with 52960 of them for the implementation of the unsupervised mechanism and the remaining 8516 for the supervised one. We empirically chose  $d = 16$  as the hidden space dimension. In line with a common empirical approach (the interested reader can refer to the TensorFlow Tutorial<sup>3</sup>, we considered the first  $d/2$  neurons as  $\mu$  vector of the means, and the remaining  $d/2$  neurons account for the variance  $\sigma^2$  vector. Incidentally, we report that we have tested the results for different values of  $d$ , specifically,  $d = 2, 4, 8, 16, 32, 64, 128$ , finding comparable results.

### 3.2 vEEGNet as Classifier

vEEGNet was used to classify the MI class for every subject in the dataset. Table 1 reports its classification performance in terms of accuracy and Cohen's  $\kappa$  score with respect to other DL models, including our previous optimized implementation of EEGNet (*DynamicNet* (Zancanaro et al., 2021)) and general-purpose CNN-based models (i.e., the CW-CNN, the DFFN, and the Monolithic network). Performance are reported for each individual subject as well as for the grand-average (i.e., mean across all subjects).

We decided to include in the comparison only those papers which reported the individual performance for all subjects for the 4-class classification. Thus, we excluded some previous works implementing CNN- or EEGNet-based architectures that either considered 2 classes or grand-average accuracy, only (e.g., (Schirrmeyer et al., 2017)). From Table 1,

<sup>2</sup>The code is available on GitHub: <https://github.com/jesus-333/Variational-Autoencoder-for-EEG-analysis>

<sup>3</sup>Available at <https://www.tensorflow.org/tutorials/generative/cvae>

it can be noticed that those models which combine multiple EEGNet *units* (e.g., TSGL-EEGNet, MB-Shallow ConvNet) can reach higher performance, in the order of 80% (despite of the type of combination, i.e., in parallel or in series), while other models achieve accuracy values in the range 71%-78%. It might be possible that this is due to the different features that each specific architecture can extract, leading to better adaptability to each individual subject. It is well-known that different subjects share similar frequency bands to realize MI, but each of them can have the strongest MI-related component at a slightly different frequency (Magnuson and McNeil, 2021; Li et al., 2018; Bressan et al., 2021). In turn, this might be the reason why models built on a single choice of frequency-domain features, i.e., including the original EEGNet, are not able to generalize well. Also, it is worth observing that most of the models, including ours, apply very basic or no pre-processing at all. MI-EEGNet is the only EEGNet-based model which invasively pre-processes the input EEG with a narrow band 4-38 Hz filter and a 50 Hz notch, reaching an accuracy value of 74.61% with very high variability across subjects (i.e., the standard deviation is 15.44%). At the individual subject level, from Table 1, we found that there exists a large inter-subject variability, as expected from the literature on EEG, with standard deviation values in the range of 6.27% to 15.44%. At the same time, it is not fully clear why the classification accuracy for some specific subjects (e.g., subject nn.3 and 7) is very high, despite the model used, while for some others the classification seems to be generally more difficult (e.g., for subject nn.2 and 6). This requires further investigations in the future to increase the adaptability and the generalization ability of these kinds of DL architectures.

### 3.3 vEEGNet as Generator

Fig. 2 reports an example of reconstructed EEG signal from channel C3 during the imagination of the

Table 1: Comparison of vEEGNet with other DL models in terms of classification accuracy (%) and kappa score (when available, its value is within brackets) in a four classes MI task. The first five columns refer to EEGNet-based models, while the last three columns refer to general-purpose CNN models. AVG stands for average, STD for standard deviation.

	vEEGNet (d = 16)	EEGNet (DynamicNet)	TSGL- EEGNet	MI-EEGNet	MBSshallow ConvNet	CW-CNN	DFFN	Monolithic Network
1	78.13 (0.71)	81.88	85.41 (0.81)	83.68 (0.78)	82.58 (0.77)	86.11 (0.82)	83.2	83.13 (0.67)
2	61.81 (0.49)	60.97	70.67 (0.61)	49.65 (0.33)	70.01 (0.6)	60.76 (0.48)	65.69	65.45 (0.35)
3	84.72 (0.8)	88.54	95.24 (0.94)	89.24 (0.86)	93.79 (0.92)	86.81 (0.82)	90.29	80.29 (0.65)
4	65.28 (0.54)	70.63	80.26 (0.74)	68.06 (0.57)	82.6 (0.77)	67.36 (0.57)	69.42	81.6 (0.62)
5	70.49 (0.61)	68.45	70.29 (0.6)	64.93 (0.53)	77.81 (0.7)	62.5 (0.5)	61.65	76.7 (0.58)
6	60.42 (0.47)	61.46	68.37 (0.58)	56.25 (0.42)	64.79 (0.53)	45.14 (0.27)	60.74	71.12 (0.45)
7	79.86 (0.73)	82.08	90.97 (0.88)	94.1 (0.92)	88.02 (0.84)	90.63 (0.88)	85.18	84 (0.69)
8	79.17 (0.72)	82.15	86.35 (0.82)	82.64 (0.77)	86.91 (0.83)	81.25 (0.75)	84.21	82.66 (0.7)
9	67.71 (0.57)	66.25	83.64 (0.79)	82.99 (0.77)	83.38 (0.78)	77.08 (0.69)	85.48	80.74 (0.64)
AVG	<b>71.95 (0.63)</b>	<b>73.60</b>	<b>81.34 (0.75)</b>	<b>74.61 (0.66)</b>	<b>81.15 (0.75)</b>	<b>73.07 (0.64)</b>	<b>76.44</b>	<b>78.1 (0.59)</b>
STD	<b>8.78 (0.12)</b>	<b>10.20</b>	<b>9.61 (0.13)</b>	<b>15.44 (0.21)</b>	<b>9.03 (0.12)</b>	<b>15.11 (0.2)</b>	<b>11.65</b>	<b>6.27 (0.12)</b>

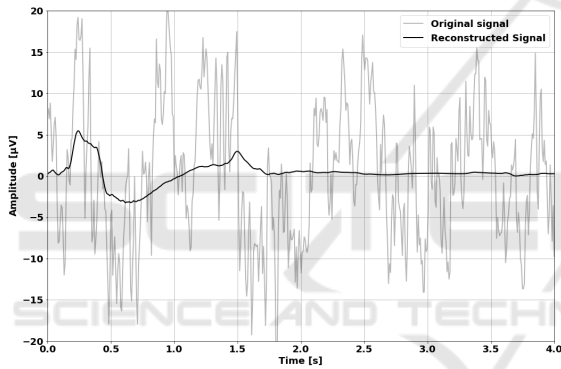


Figure 2: An example of reconstructed EEG (channel C3).

right-hand movement. At a first sight, the reconstruction seems not to be successful and poorly consistent with the original signal. However, we might recognize in the reconstructed signal a specific EEG component that typically appears, following a precise timing, when a movement is executed or imagined, the so-called MRCP. MRCPs are low-frequency components (typically in the  $\delta$  or  $\theta$  bands, i.e., in the range 0.5-4 Hz) that are characterized by a sequence of positive and negative peaks after the "GO" cue (i.e., the time zero in our case) (Magnuson and McNeil, 2021).

Fig. 3 shows four different reconstructed EEG channels, namely C3, C4, Cz, and the average of FC3 and FC4, selected based on their relevance to the MI tasks. To be specific, in line with well-known literature (Lazurenko et al., 2018), the most relevant electrodes where to retrieve information related to the hand movement are the contralateral central sensors C3 and C4, for the right and the left-hand movements, respectively, while for the legs is Cz, and for

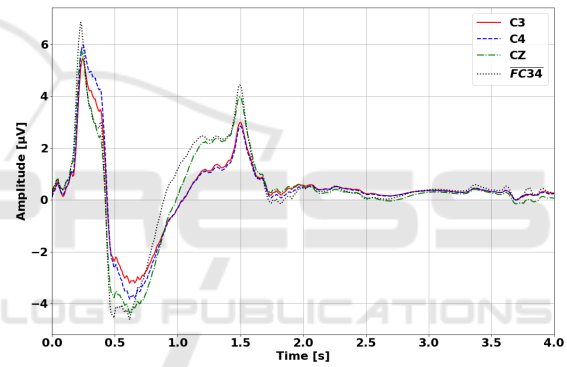


Figure 3: Reconstructed channels C3, C4, Cz, and average FC3 and FC4.

the tongue are the frontal sensors F3 and F4 (with a prevalence of F3). In our dataset, F3 and F4 were not available, then we considered the nearest available sensors which were FC3 and FC4 (as in the International 10-20 System for EEG electrode placement). If Fig. 3 is compared with the consolidated literature on MRCP during motor execution and imagery (Magnuson and McNeil, 2021; Li et al., 2018; Bressan et al., 2021), we might recognize a very similar pattern: a positive peak occurs right after the "GO" cue, then a negative peak follows (before 1 s), and finally a rebound is observed. The entire waveform almost expires (i.e., returns to baseline) within approximately 2 s after the cue. Here, we could observe a pattern that is very consistent with the expected one. Therefore, we can conclude that vEEGNet is extracting a compact representation of a multi-channel EEG that represents its lower frequency component during the MI. This allows the model to obtain satisfactory accu-

racy values in the classification of 4 different MI tasks and to extract an MRCP pattern. However, this speculation needs to be confirmed with further analysis and investigations. Also, in the future, it might be worth providing further explanations, in line with (Zoppis et al., 2020; Scapin et al., 2022), of the mechanisms that the DL models process the EEG signals, and how to drive the architecture to reconstruct not only the slower components of the signal (e.g., the MRCPs) but also the faster ones (e.g., the  $\mu$  and  $\beta$  components ranging between 8 and 30 Hz) (Pfurtscheller et al., 2006).

## 4 CONCLUSIONS

In this work, we tackled the challenging problem of the multi-class classification of different MI tasks using EEG. Several ML and DL models have been proposed to solve this complex problem. Among others, EEGNet by (Lawhern et al., 2016) and its several variants gained a lot of attention in the last few years, since 2016. However, these models typically provide medium to high accuracy values (between 70% and 80% approximately), but can poorly explain how they decide on the classification output. Therefore, in this work, we proposed a new DL model, namely vEEGNet, whose objective is two-fold: the model is used to classify EEG signals during participants' MI (i.e., of a hand, the feet, or the tongue); at the same time, it is enriched by a module that is able to reconstruct the EEG. In vEEGNet, we employed an EEGNet to encode a multi-channel EEG dataset, and to extract a latent representation in e.g., 16 dimensions. Then, a mirrored version of EEGNet is used to decode such compact representation into a new synthetically generated multi-channel EEG. In parallel, a FFNN takes in input newly generated EEG samples from the latent representation and uses them to recognize one out of four different imagined movements. We show that vEEGNet is able to classify the EEG with performances that are comparable with the state of the art. Interestingly, we also found out that the reconstructed signals resemble some specific, and well-known, EEG components that are strongly related to MI, the MRCPs. Thus, this paper presents a new architecture that has the potentiality to both classify EEG during MI as well as provide a link between neurophysiology and the model's classification decisions. Although vEEGNet, in its current implementation, cannot significantly outperform other models, it is worth highlighting that it was built on top of the standard EEGNet (implemented in our DynamicNet framework (Zancanaro et al., 2021)) and it

can achieve its reference state-of-the-art performance, i.e., the fairest comparison being with EEGNet itself which - in fact - reached a very close average accuracy value, slightly exceeding 70%, across the subjects. Thus, at present, we could not obtain a clear advantage in terms of classification accuracy in having also trained the model on the reconstruction term. This is one of the limitations of this contribution. There are also other aspects that will deserve further investigation. Particularly, it might be worth exploring, at least, two different directions: on one side, optimizing the overall loss function by better balancing its two main contributions (i.e., the VAE loss function and the classification loss function) might lead to a performance improvement. On the other hand, another DL model, which can reach higher accuracies in its basic architecture compared to the standard EEGNet (e.g., MBSshallow ConvNet), might be used to implement the encoder of vEEGNet to test if performances increase in our more general-purpose architecture. Another way to improve this work, and explain the vEEGNet model performance in both classification and reconstruction, as well as their mutual relationship, is to study the different behavior of the model in response to modifications of the input (as in some explainability studies where ablation, permutation or other kinds of perturbations have been applied to the EEG input (Manjunatha and Esfahani, 2021)), towards a more transparent and explainable DL approach. Finally, modifications of the architecture could be adopted to extract different features and also reconstruct faster components that can be relevant to the MI task, e.g., the  $\alpha$  and  $\beta$  frequencies in the range 8 to 30 Hz (as well-established by previous literature (Pfurtscheller et al., 2006)). Besides, vEEGNet could be used to deepen into the problem of the inter-subject variability that typically prevents DL models to be easily generalized from subject to subject (and even experimental session to session of the same subject). This might be of such an impact in the field of, e.g., BCI, where the system needs to seamlessly interact with patients and healthy naïve users. Finally, future investigations of the potentialities of vEEGNet as a generative model for EEG can be addressed to cope with the common lack of large EEG datasets that make it difficult for DL models to improve their performance and better generalize.

## ACKNOWLEDGEMENTS

AZ is supported by PON 2014-2020 action IV.4 funded by the Italian Ministry of University and Research at the University of Padova (Padova, Italy).

GC is supported by PON Initiative 2014-2020 action IV.6 funded by the Italian Ministry of University and Research at the University of Milan-Bicocca (Milan, Italy).

## REFERENCES

- Altuwajri, G. A. and Muhammad, G. (2022). A multi-branch of convolutional neural network models for electroencephalogram-based motor imagery classification. *Biosensors*, 12(1).
- Beraldo, G., Tonin, L., Millán, J. d. R., and Menegatti, E. (2022). Shared intelligence for robot teleoperation via BMI. *IEEE Transactions on Human-Machine Systems*.
- Blankertz, B., Dornhege, G., Krauledat, M., Müller, K.-R., and Curio, G. (2007). The non-invasive Berlin Brain-Computer Interface: Fast acquisition of effective performance in untrained subjects. *NeuroImage*, 37:539–50.
- Blei, D. M., Kucukelbir, A., and McAuliffe, J. D. (2017). Variational inference: A review for statisticians. *Journal of the American statistical Association*, 112(518):859–877.
- Bressan, G., Cisotto, G., Müller-Putz, G. R., and Wriessneger, S. C. (2021). Deep learning-based classification of fine hand movements from low frequency eeg. *Future Internet*, 13(5):103.
- Cisotto, G., Capuzzo, M., Guglielmi, A. V., and Zanella, A. (2022). Feature stability and setup minimization for EEG-EMG-enabled monitoring systems. *EURASIP Journal on Advances in Signal Processing*, 2022(1):103.
- Deng, X., Zhang, B., Yu, N., Liu, K., and Sun, K. (2021). Advanced TSGL-EEGNet for motor imagery EEG-based Brain-Computer Interfaces. *IEEE Access*, 9:25118–25130.
- Hinton, G. E. and Salakhutdinov, R. R. (2006). Reducing the dimensionality of data with neural networks. *science*, 313(5786):504–507.
- Kai Keng Ang, Zheng Yang Chin, Haihong Zhang, and Cuntai Guan (2008). Filter bank common spatial pattern (FBCSP) in Brain-Computer Interface. In *2008 IEEE Int. Joint Conf. on Neural Networks (IEEE World Congress on Computational Intelligence)*.
- Kingma, D. P. and Welling, M. (2013). Auto-encoding variational bayes. *arXiv preprint arXiv:1312.6114*.
- Lawhern, V., Solon, A., Waytowich, N., Gordon, S., Hung, C., and Lance, B. (2016). EEGNet: A compact convolutional network for EEG-based Brain-Computer Interfaces. *Journal of Neural Engineering*, 15.
- Lazurenko, D., Kirov, V., Aslanyan, E., Shepelev, I., Bakhtin, O., and Minyaeva, N. (2018). Electrographic properties of movement-related potentials. *Neuroscience and Behavioral Physiology*, 48(9):1078–1087.
- Li, D., Wang, J., Xu, J., and Fang, X. (2019a). Densely feature fusion based on convolutional neural networks for motor imagery EEG classification. *IEEE Access*, 7:132720–132730.
- Li, H., Huang, G., Lin, Q., Zhao, J.-L., Lo, W.-L. A., Mao, Y.-R., Chen, L., Zhang, Z.-G., Huang, D.-F., and Li, L. (2018). Combining movement-related cortical potentials and event-related desynchronization to study movement preparation and execution. *Frontiers in neurology*, 9:822.
- Li, Y., Pan, Q., Wang, S., Peng, H., Yang, T., and Cambria, E. (2019b). Disentangled variational auto-encoder for semi-supervised learning. *Information Sciences*, 482:73–85.
- Loshchilov, I. and Hutter, F. (2019). Decoupled weight decay regularization. In *International Conference on Learning Representations*.
- Magnuson, J. R. and McNeil, C. J. (2021). Low-frequency neural activity at rest is correlated with the movement-related cortical potentials elicited during both real and imagined movements. *Neuroscience Letters*, 742:135530.
- Manjunatha, H. and Esfahani, E. T. (2021). Extracting interpretable eeg features from a deep learning model to assess the quality of human-robot co-manipulation. In *2021 10th International IEEE/EMBS Conference on Neural Engineering (NER)*, pages 339–342. IEEE.
- Olivas, B. E. and Chacon, M. (2018). Classification of multiple motor imagery using deep convolutional neural networks and spatial filters. *Applied Soft Computing*, 75.
- Pfurtscheller, G., Brunner, C., Schlögl, A., and Da Silva, F. L. (2006). Mu rhythm (de) synchronization and EEG single-trial classification of different motor imagery tasks. *NeuroImage*, 31(1):153–159.
- Riyad, M., Khalil, M., and Adib, A. (2021). MI-EEGNET: A novel convolutional neural network for motor imagery classification. *Journal of Neuroscience Methods*, 353:109037.
- Sakhavi, S., Guan, C., and Yan, S. (2018). Learning temporal information for brain-computer interface using convolutional neural networks. *IEEE Transactions on Neural Networks and Learning Systems*, 29(11):5619–5629.
- Scapin, D., Cisotto, G., Gindullina, E., and Badia, L. (2022). Shapley value as an aid to biomedical machine learning: a heart disease dataset analysis. In *2022 22nd IEEE International Symposium on Cluster, Cloud and Internet Computing (CCGrid)*, pages 933–939. IEEE.
- Schirrmester, R. T., Springenberg, J. T., Fiederer, L. D. J., Glasstetter, M., Eggensperger, K., Tangermann, M., Hutter, F., Burgard, W., and Ball, T. (2017). Deep learning with convolutional neural networks for EEG decoding and visualization. *Human Brain Mapping*.
- Schneider, T., Wang, X., Hersche, M., Cavigelli, L., and Benini, L. (2020). Q-EEGNet: An energy-efficient 8-bit quantized parallel EEGNet implementation for edge motor-imagery brain-machine interfaces. In *2020 IEEE International Conference on Smart Computing (SMARTCOMP)*, pages 284–289. IEEE.

- Zancanaro, A., Cisotto, G., Paulo, J. R., Pires, G., and Nunes, U. J. (2021). CNN-based approaches for cross-subject classification in motor imagery: From the state-of-the-art to DynamicNet. In *2021 IEEE Conference on Computational Intelligence in Bioinformatics and Computational Biology (CIBCB)*, pages 1–7.
- Zancanaro, A., Cisotto, G., Tegegn, D. D., Manzoni, S. L., Reguzzoni, I., Lotti, E., and Zoppis, I. (2022). Variational autoencoder for early stress detection in smart agriculture: A pilot study. In *2022 IEEE Workshop on Metrology for Agriculture and Forestry (MetroAgriFor)*, pages 126–130. IEEE.
- Zoppis, I., Zanga, A., Manzoni, S., Cisotto, G., Morreale, A., Stella, F., and Mauri, G. (2020). An attention-based architecture for eeg classification. In *BIOSIGNALS*, pages 214–219.

